nature photonics

LETTERS

PUBLISHED ONLINE: 13 APRIL 2014 | DOI: 10.1038/NPHOTON.2014.57

Coherent terabit communications with microresonator Kerr frequency combs

Joerg Pfeifle[1], Victor Brasch[2], Matthias Lauermann[1], Yimin Yu[1], Daniel Wegner[1], Tobias Herr[2], Klaus Hartinger[3], Philipp Schindler[1], Jingshi Li[1], David Hillerkuss[1†], Rene Schmogrow[1], Claudius Weimann[1], Ronald Holzwarth[3], Wolfgang Freude[1], Juerg Leuthold[1†], Tobias J. Kippenberg[2]* and Christian Koos[1]*

Optical frequency combs have the potential to revolutionize terabit communications[1]. The generation of Kerr combs in nonlinear microresonators[2] is particularly promising[3], enabling line spacings of tens of gigahertz. However, such combs may exhibit strong phase noise[4–6], which has made high-speed data transmission impossible up to now. Here, we demonstrate that systematic adjustment of the pump conditions for low phase noise[4,7–9] enables coherent data transmission with advanced modulation formats that pose stringent requirements on the spectral purity of the comb. In a first experiment, we encode a data stream of 392 Gbit s^{-1} on a Kerr comb using quadrature phase-shift keying and 16-state quadrature amplitude modulation. A second experiment demonstrates feedback stabilization of the comb and transmission of a 1.44 Tbit s^{-1} data stream over up to 300 km. The results show that Kerr combs meet the highly demanding requirements of coherent communications and thus offer an attractive route towards chip-scale terabit-per-second transceivers.

Optical interconnects providing data rates of multiple terabits per second are the most promising option for overcoming transmission bottlenecks in warehouse-scale data centres and worldwide communication networks. By using highly parallel wavelength division multiplexing (WDM) with tens or hundreds of channels in combination with spectrally efficient advanced modulation formats, transmission capacity of multiple terabits per second can be achieved while keeping symbol rates compliant with the electrical bandwidth of energy-efficient CMOS driver circuitry[10,11]. The silicon platform lends itself to integration of the associated photonic–electronic interfaces using large-scale fabless CMOS processing[12,13]. While integrated terabit-per-second WDM receivers have already been demonstrated[14], scalability of the transmitter capacity is still limited by a lack of adequate optical sources, especially when using advanced modulation formats that encode information on both the amplitude and the phase of the optical wave and therefore require optical carriers with particularly low phase and amplitude noise.

Optical carriers for WDM transmission are commonly generated by distributed feedback (DFB) laser arrays. Chip-scale transmitter systems with DFB lasers have been realized on InP substrates, showing potential for simultaneous operation of 40 channels[15]. However, these approaches cannot be transferred directly to the silicon photonic platform, as combining conventional DFB laser arrays with silicon photonic transmitters would require a multitude of chip–chip interfaces, thereby significantly increasing the packaging effort. Hybrid integration of III–V dies on silicon substrates[16] avoids these interfaces, but scalability to large channel counts is still limited by the gain bandwidth of the semiconductor material and by thermal constraints. Moreover, the spectral efficiency of DFB-based transmission systems suffers from the uncertainty of the individual emission frequencies, which is of the order of several gigahertz and requires appropriate guard bands to avoid spectral overlap of neighbouring WDM channels. For dense WDM with a channel spacing of, for example, 25 GHz, the guard bands consume a significant fraction of the available transmission bandwidth.

These limitations can be overcome by exploiting optical frequency combs as sources for WDM transmission. Frequency combs consist of a multitude of equidistant spectral lines, each of which can be modulated individually[1,17,18]. The inherently constant frequency spacing of the comb lines enables the transmission of orthogonal frequency-division multiplexing (OFDM) signals[1] or of Nyquist-WDM signals[18] with closely spaced subcarriers. Frequency combs with line spacings in the gigahertz range can be generated by external modulation of a narrowband continuous-wave (c.w.) signal[19], by mode-locked lasers based on semiconductor quantum-dot or quantum-dash materials[20], or by exploiting parametric frequency conversion in Kerr-nonlinear high-Q microcavities[2]. In contrast to modulator-based approaches or mode-locked laser diodes, the bandwidth of Kerr combs is neither limited by the achievable modulation depth nor by the gain bandwidth of the active medium. Kerr combs can therefore exhibit bandwidths of hundreds of nanometres[21], thereby covering multiple telecommunication bands (such as the C, L and U bands) with typical line spacings between 10 GHz and 100 GHz.

Kerr comb generation has been demonstrated using various different technology platforms[21], including silica[2], calcium fluoride (CaF_2)[22], Hydex glass[23] or silicon nitride (Si_3N_4)[24]. Previous experiments have used such devices for data transmission with conventional 10 Gbit s^{-1} or 40 Gbit s^{-1} on–off keying as the modulation format[3,5,6]. However, Kerr frequency combs tend to exhibit multiple spectral lines within a single resonance, leading to strong amplitude fluctuations and phase noise[4,5]. Such fluctuations are prohibitive for spectrally efficient data transmission with advanced modulation formats. Although low-phase-noise Kerr combs have been demonstrated recently[4,7–9], coherent transmission with Kerr combs has not yet been shown.

Here, we report the first experimental demonstration of coherent data transmission with amplitude- and phase-modulated carriers

[1]Institute of Photonics and Quantum Electronics (IPQ) and Institute of Microstructure Technology (IMT), Karlsruhe Institute of Technology (KIT), 76131 Karlsruhe, Germany, [2]École Polytechnique Fédérale de Lausanne (EPFL), 1015 Lausanne, Switzerland, [3]Menlo Systems GmbH, 82152 Martinsried, Germany, [†]Present address: Electromagnetic Fields & Microwave Electronics Laboratory (IFH), ETH Zurich, 8092 Zurich, Switzerland.
*e-mail: tobias.kippenberg@epfl.ch; christian.koos@kit.edu

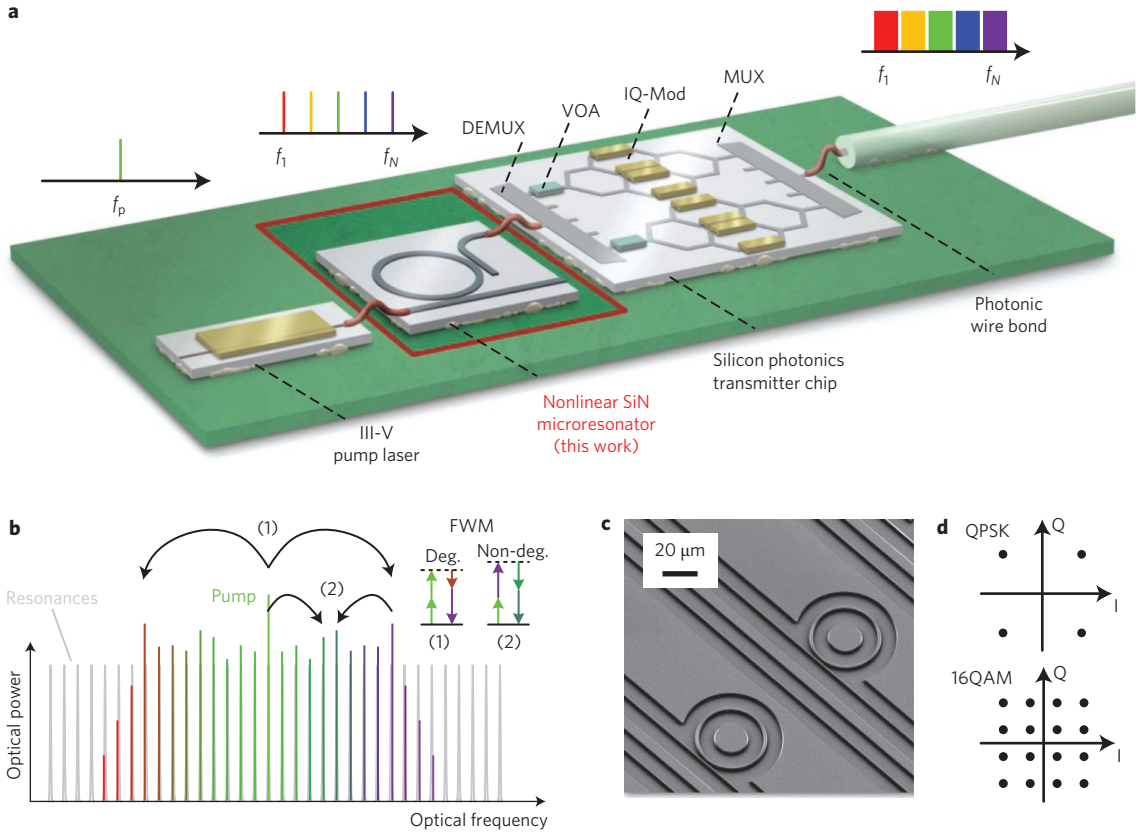

Figure 1 | Principles of coherent terabit-per-second communications with Kerr frequency combs. a, Artist's view of a future chip-scale terabit-per-second transmitter, leveraging a Kerr frequency comb source. The demonstration of coherent data transmission with Kerr combs is the subject of this work. DEMUX, de-multiplexer; VOA, variable optical attenuator; IQ-Mod, IQ-modulator; MUX, multiplexer. **b**, Illustration of Kerr comb formation by multi-stage FWM. Degenerate FWM (1) converts two photons at the pump frequency to a pair of photons that are up- and downshifted in frequency, whereas cascaded non-degenerate FWM (2) populates the remaining resonances. **c**, SEM image of an integrated high-*Q* SiN microresonator. High-index-contrast SiN waveguides enable dense integration. **d**, Constellation diagrams of QPSK and 16QAM signals, where information is encoded both in the amplitude and the phase of the optical carrier, which can be represented by the in-phase (I, horizontal axis) and quadrature (Q, vertical axis) components of the complex electrical field amplitude.

derived from a Kerr frequency comb. Coherent transmission allows both the information content and the data rate to be increased, but it also places stringent requirements on the phase and amplitude stability of the optical carrier. Our experiments build on systematic investigations of comb formation dynamics[4] to generate highly stable Kerr combs with low phase noise. We encode uncorrelated data on neighbouring comb lines using quadrature phase-shift keying (QPSK) and 16-state quadrature amplitude modulation (16QAM) in combination with Nyquist pulses that have nearly rectangular power spectra and provide highest spectral efficiency. In a first experiment, we use polarization multiplexing and a symbol rate of 14 GBd on five QPSK channels and one 16QAM channel to obtain an aggregate data rate of 392 Gbit s^{-1}. This corresponds to a net spectral efficiency of 6 bit s^{-1} Hz^{-1} (3 bit s^{-1} Hz^{-1}) for the 16QAM (QPSK) channels. In a second experiment, we boost the data rate to 1.44 Tbit s^{-1}, encoded on 20 neighbouring comb lines and transmitted over a distance of 300 km. The comb is stabilized by a feedback loop that controls the pump wavelength. The results clearly demonstrate the large potential of Kerr frequency combs for future chip-scale terabit-per-second communication systems. As an integration platform for the comb source we chose SiN, because of its reliability and its compatibility with CMOS processing[24].

Our vision of a future chip-scale terabit-per-second transmitter is illustrated in Fig. 1a. A Kerr frequency comb is generated by exploiting multi-stage four-wave mixing (FWM) in a high-*Q* Kerr-nonlinear microresonator pumped with a strong c.w. laser[2,21]. The envisaged transmitter consists of a multi-chip assembly, with single-mode photonic wire bonds[25] connecting the individual chips. In contrast to monolithic integration, this hybrid approach allows the advantages of different photonic integration platforms to be combined: for the optical pump, III–V semiconductors can be used[15], while the high-*Q* ring resonator for Kerr comb generation could be fabricated using, for example, low-loss SiN waveguides[24]. The optical carriers are separated and individually modulated on a transmitter chip, with large-scale silicon photonic integration lending itself to particularly compact and energy-efficient multiplexing (MUX) and de-multiplexing (DEMUX) filters[13] and IQ modulators[26,27].

Figure 1b illustrates the basic principle of Kerr comb generation. Pump energy is transferred to the comb lines by two processes: degenerate FWM, indicated by (1) in Fig. 1b, leads to the formation of two side modes by converting two pump photons into a pair of photons that are up- and downshifted in frequency. The magnitude of the frequency shift is determined by the pump power and cavity dispersion[4]; a multitude of cascaded non-degenerate FWM processes, indicated by (2) in Fig. 1b, fully populate the remaining resonances. Kerr comb generators can be extremely compact, see Fig. 1c, which shows a scanning electron microscope (SEM) image of a planar integrated SiN microresonator.

To maximize the spectral efficiency we used advanced modulation formats that encode data both on the amplitude and the

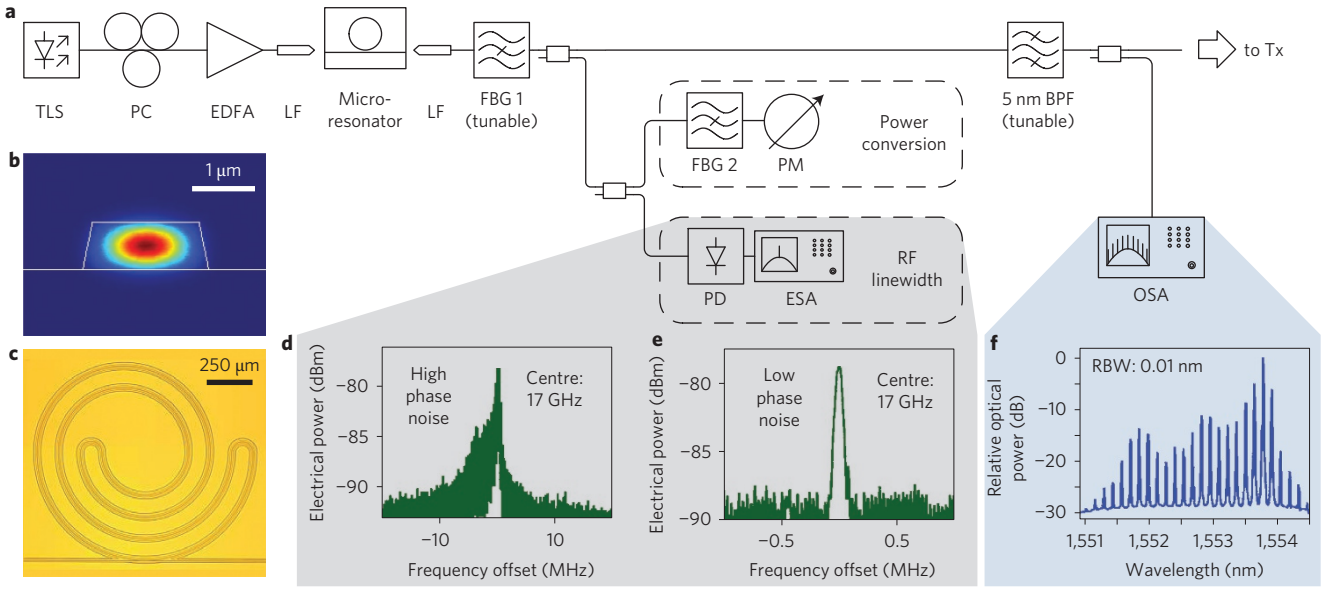

Figure 2 | Comb generation set-up. a, The optical pump comprises a tunable laser source (TLS), a polarization controller (PC) and an erbium-doped fibre amplifier (EDFA). Lensed fibres (LF) couple light to and from the microresonator chip. A fibre Bragg grating (FBG 1) serves as a tunable narrowband notch filter to suppress residual pump light. For adjustment of the pump parameters, we monitor the power conversion from the pump to the adjacent lines (PM, power meter). An electronic spectrum analyser (ESA) is used to measure the RF linewidth in the photocurrent spectrum of the photodetector (PD). A 5-nm-wide spectral section is extracted from the comb spectrum and used for data transmission. **b**, Waveguide cross-section and mode profile. **c**, Optical micrograph of the resonator. **d**, RF spectrum of a high phase-noise comb state (RBW = 10 kHz). **e**, RF spectrum of a low phase-noise comb state (RBW = 30 kHz). **f**, Selected part of the comb spectrum (OSA, optical spectrum analyser). RBW, resolution bandwidth.

phase of each comb line. This is illustrated in Fig. 1d for QPSK and 16QAM. The complex electric field of the data signal is visualized by its in-phase (I, horizontal axis) and quadrature component (Q, vertical axis) in the complex plane. For QPSK, the I- and Q-components can assume two distinct values, leading to four signal states (symbols) in the complex plane. This represents an information content of two bits per symbol. Similarly, a 16QAM symbol can assume 16 states in the complex plane, corresponding to four bits of information per symbol. A densely packed optical signal spectrum, as schematically depicted in the upper right corner of Fig. 1a, can be achieved by using sinc-shaped Nyquist pulses with rectangular power spectra[28].

The viability of the concept illustrated in Fig. 1 was demonstrated in a proof-of-principle experiment with discrete photonic components. Kerr combs were generated with the set-up depicted in Fig. 2a. To this end, pump light from a narrow-linewidth tunable laser source (TLS) is adjusted in polarization and amplified by an erbium-doped fibre amplifier (EDFA). Lensed fibres (LF) couple the light into a Si_3N_4 resonator with a free spectral range (FSR) of 17 GHz (Fig. 2). Figure 2b shows the waveguide cross-section of the resonator and the calculated mode profile. The ring resonator waveguide is coiled up to reduce the footprint and exhibits a loaded Q-factor of 8×10^5. In contrast to the concept illustrated in Fig. 1, our experiments relied on comb generators with a single waveguide to couple pump light to the resonator and to extract the frequency comb. As a consequence, strong c.w. pump light can pass through the resonator and needs to be suppressed by a tunable fibre Bragg grating (FBG 1) at the output of the device. It has recently been shown that the stability and phase noise of the Kerr comb are closely linked to the pump conditions[4]. Careful tuning of pump power, frequency and polarization is therefore of prime importance. To adjust these parameters in the experiment we used two optimization criteria: the power of the newly generated comb lines measured behind a second fibre Bragg grating, FBG 2, and the radiofrequency (RF) linewidth measured using a photodetector, PD, and electrical spectrum analyser, ESA. A more detailed description of the adjustment of the pump parameters can be found in the Methods.

For data transmission, a 5-nm-wide spectral section was extracted from the comb using an optical bandpass filter (BPF), see Fig. 2f for the corresponding spectrum. The carriers were modulated with QPSK and 16QAM signals at a symbol rate of 14 GBd. To enable dense packing of optical channels and to maximize the spectral efficiency, we used sinc-shaped Nyquist pulses with rectangular power spectra[28]. We transmitted data streams on two orthogonal polarizations of a standard single-mode fibre (polarization-division multiplexing). The signal was detected with a commercial optical modulation analyser using a tunable laser as a local oscillator. The experimental set-up for data transmission and SiC digital post-processing techniques are described in more detail in the Supplementary Section II.

The results of the data transmission experiment are summarized in Fig. 3. Figure 3a depicts the optical power spectrum of the modulated carriers for all six data channels. We did not flatten the comb spectrum before modulation to compare the influence of different carrier powers on the transmission performance. As a quantitative measure of signal quality, we used the error vector magnitude (EVM), which describes the effective distance of a received complex symbol from its ideal position in the constellation diagram. When using a standard forward error-correction (FEC) scheme with 7% overhead, the limits for error-free detection are given by an EVM of 38% (11%) for QPSK (16QAM) (see Supplementary Section II and references therein). The constellation diagrams for each polarization of the six wavelength channels are depicted in Fig. 3b together with the measured EVM. All channels are well below the 38% threshold for QPSK, and channel 5 even shows a sufficiently good performance for 16QAM transmission. We transmitted with a symbol rate of 14 GBd and chose QPSK for channels 1–4 and 6, and 16QAM for channel 5. Taking into account polarization multiplexing, we obtained an aggregate data rate of 392 Gbit s^{-1}. Considering the overhead of 7% for FEC, the net spectral efficiency amounts to 3 bit s^{-1} Hz^{-1} for the QPSK and 6 bit s^{-1} Hz^{-1} for the 16QAM channels.

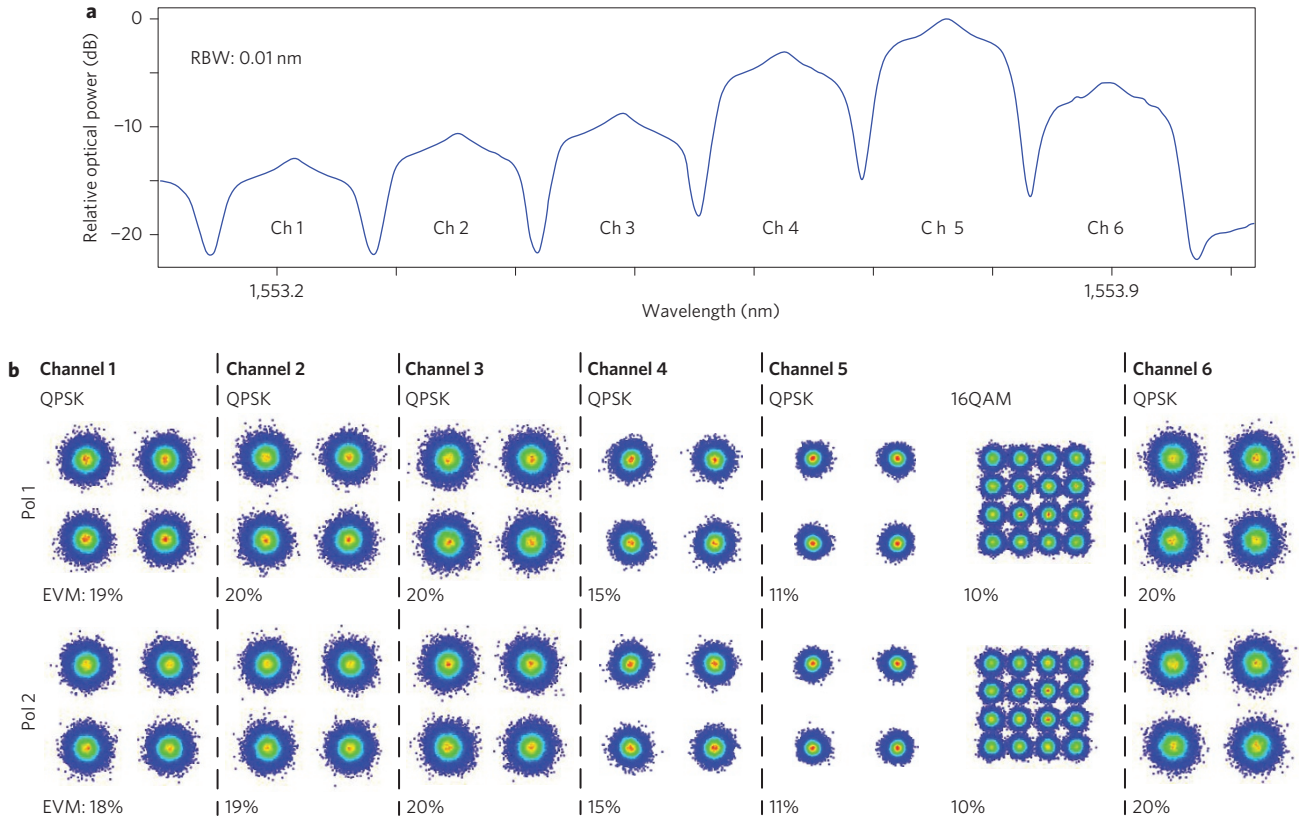

Figure 3 | Coherent data transmission using a Kerr microresonator frequency comb. a, Spectrum of modulated carriers for all six data channels, measured at the input of the OMA. **b**, Constellation diagrams for each channel and for both polarizations, as well as the corresponding error vector magnitude (EVM). The constellation diagrams show no sign of excessive phase noise, which would result in constellation points that are elongated along the azimuthal direction. For QPSK, the BER of all channels is below 4.5×10^{-3}, which corresponds to an EVM of 38%; for channels 4 and 5 the BER is even smaller than 1×10^{-9} (EVM < 16.7%). The good quality of channel 5 enables transmission of a 16QAM signal with a measured BER of 7.5×10^{-4}.

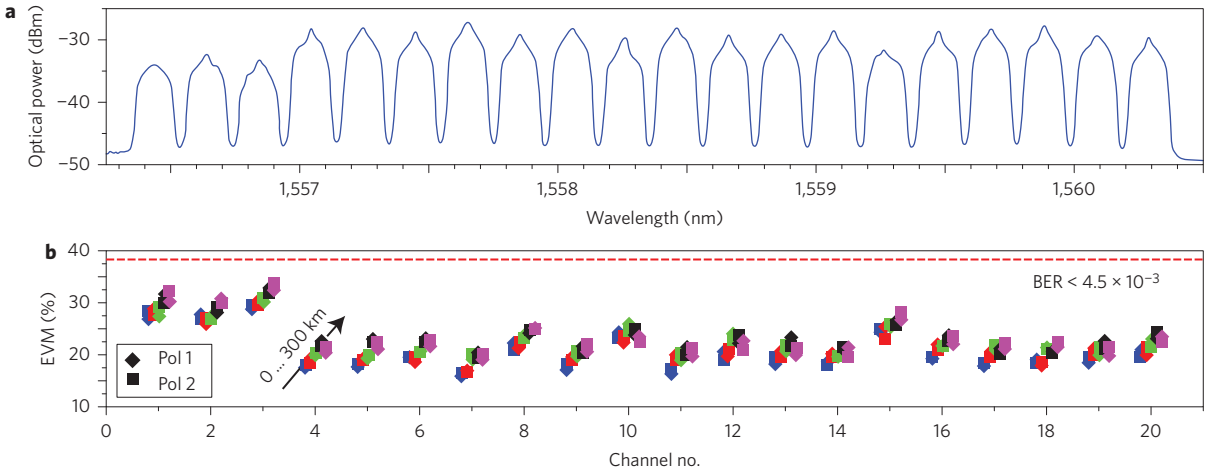

Figure 4 | Coherent terabit-per-second data transmission using a feedback-stabilized Kerr frequency comb. a, Optical spectrum of the 1.44 Tbit s^{-1} data stream. The spectrum was flattened before modulation. **b**, EVM for all data channels and fibre spans. The carriers are modulated at a symbol rate of 18 GBd using QPSK and Nyquist pulse shaping. Using polarization multiplexing at each of the 20 WDM channels, an aggregate data rate of 1.44 Tbit s^{-1} is achieved. The polarizations are distinguished by diamonds and squares, while the different fibre spans (0 km, 75 km, 150 km, 225 km, 300 km) are colour-coded and slightly offset in the horizontal direction, as indicated by the arrow. The red dashed line indicates an EVM of 38%, which corresponds to the BER threshold for second-generation FEC.

When relating the EVM to the bit error ratio (BER), we assumed that the signal was impaired by additive white Gaussian noise. The validity of this assumption is supported by the fact that the deviations of the measured from the ideal constellation points occur equally in all directions and do not show any sign of anisotropy. Excessive phase noise, in particular, can be excluded as a relevant impairment of data transmission as this would lead to constellation points that are elongated along the azimuthal direction. Instead, the

signal impairments can be attributed to strong amplified spontaneous emission (ASE) originating from the high-power pump EDFA. In the current configuration, ASE light passes straight through the resonator chip and superimposes the comparatively weak comb lines as additive white Gaussian noise (see Supplementary Section III for a more detailed discussion). The results indicate that Kerr combs are indeed perfectly suited for data transmission with phase-sensitive modulation formats.

In a second experiment, we used a resonator with an FSR of 25 GHz and a Q-factor of 2×10^6, which is higher than the Q-factor in the first experiment. This allowed the pump power to be reduced to a level where filtering of the ASE noise from the EDFA was possible. To enable stable long-term operation of the Kerr comb for extended data transmission experiments, we implemented a feedback loop, which locked the wavelength of the pump laser to a specified position within the resonance of the cavity (see Methods and Supplementary Section I for more details). In contrast to the previous experiment, we now flattened the comb lines before modulation using a programmable filter. For data transmission we used QPSK at a symbol rate of 18 GBd, and we inserted up to four fibre spans of 75 km length between the transmitter and the receiver. The results are summarized in Fig. 4. We obtained 20 channels with an EVM below the threshold of 38%. The total data stream amounted to 1.44 Tbit s^{-1} with a net spectral efficiency of 2.7 bit s^{-1} Hz^{-1}. This is the highest data rate that has ever been transmitted using a Kerr comb as the WDM source.

In summary, we have demonstrated that Kerr frequency combs are well suited for high-capacity data transmission with phase-sensitive modulation formats. We show error-free transmission with data rates up to 1.44 Tbit s^{-1}, spectral efficiencies up to 6 bit s^{-1} Hz^{-1} and transmission distances up to 300 km. The received signals exhibit no sign of excessive phase noise. Assuming that the demonstrated spectral efficiency of 6 bit s^{-1} Hz^{-1} can be maintained over the entire bandwidth of the Kerr comb, we envision chip-scale transmitters providing aggregate data rates beyond 100 Tbit s^{-1}, only limited by nonlinear effects in the single-mode silica fibres used for transmission[29]. We believe that the combination of chip-scale Kerr frequency comb sources with large-scale silicon photonic integration can become a key concept for power-efficient optical interconnects, providing transmission rates that have hitherto been considered impossible.

Methods

Experimental set-up and resonator design. The pump for Kerr comb generation was generated by an external-cavity laser (New Focus Velocity Model TLB-6728), a polarization controller and an EDFA, providing an output power of up to 37 dBm, see Fig. 2. The coupling loss between the lensed fibre and the Si_3N_4 chip amounted to ~3 dB per facet. In both data transmission experiments we pumped a resonance near 1,549.4 nm. The tunable fibre Bragg grating (FBG 1) at the output of the device suppressed the remaining c.w. pump wave by ~20 dB. The ring resonator consisted of nearly stoichiometric Si_3N_4 grown in multiple layers with intermediate annealing steps[24]. The strip waveguides were patterned with electron-beam lithography and transferred to the substrate by reactive ion etching with SF_6/CH_4 chemistry. After etching, the structures were embedded into a SiO_2 cladding using low-pressure chemical vapour deposition (LPCVD). The resultant waveguides were 2 μm wide and 750 nm high, and the sidewalls inclined by 12° with respect to the vertical (Fig. 2b).

The high-temperature growth technique used to fabricate the 750-nm-thick layers of stoichiometric Si_3N_4 required annealing at 1,200 °C. This makes it difficult to fabricate SiN resonators in the framework of standard CMOS processes. One option to overcome this limitation is to use dedicated fabrication processes and multi-chip integration, as illustrated in Fig. 1. Alternatively, it is possible to deposit Si_3N_4 at 400 °C and to use ultraviolet thermal processing at lower temperatures to reduce the defect density. Both techniques are subject to ongoing research.

In the first data transmission experiment, the resonator exhibited an FSR of 17 GHz and a loaded Q-factor of 8×10^5. Kerr combs were generated using an on-chip pump power of ~33 dBm. For the second experiment, we fabricated a resonator with an FSR of 25 GHz, which exhibited an increased Q-factor of 2×10^6. The comb was generated with ~29 dBm of on-chip pump power, and the measured line spacing deviated by less than 6 MHz from the designed 25 GHz. We expect that microresonators with further improved Q-factors will enable the generation of broadband frequency combs with hundreds of lines that cover optical bandwidths of hundreds of nanometres, a multiple of what can be achieved with state-of-the-art DFB WDM laser arrays in InGaAsP technology.

In the first transmission experiment, ASE originating from the high-power pump EDFA was identified as the main source of signal impairment. To improve the signal quality, it is possible to filter out ASE using a bandpass filter before the resonator chip, as demonstrated in the second experiment. This was possible in the second experiment only, because we did not have any filters that could safely handle the 37 dBm of pump power immediately after the pump EDFA in the first experiment. In future configurations, the comb may be extracted by a second waveguide coupled to the microresonator, as illustrated in Fig. 1. This would avoid direct transmission of broadband ASE noise through the resonator device and could therefore replace any additional ASE filters. Moreover, a second waveguide coupled to the resonator would also render the FBG for pump light suppression superfluous, as direct through-coupling of strong c.w. pump light is not possible.

Pumping schemes for low-phase-noise Kerr combs. To obtain low-phase-noise Kerr combs, the pump parameters were adjusted in two steps using the set-up depicted in Fig. 2a. First, the pump wavelength was scanned periodically across the resonance at a frequency of ~100 Hz, while remaining within the stop band of FBG 2 and continuously measuring the power conversion to the spectral region outside the stop band. During these scans, the polarization of the pump signal was varied slowly to maximize the conversion. Maintaining this polarization, the detuning of the pump signal with respect to the resonance wavelength was then carefully adjusted until the initially broad RF spectrum (Fig. 2d) exhibited a single narrow peak (Fig. 2e). Note that the frequency axes of Fig. 2d,e have different scales. For an on-chip pump power of ~33 dBm, the essential part of the optical comb spectrum is depicted in Fig. 2f. The comb lines for the first data transmission experiment were selected from this partial spectrum. Spectra of the comb used for the second experiment can be found in the Supplementary Section I.

The on-chip pump power needed for Kerr comb generation in the first and second experiments still amounted to 33 dBm and 29 dBm, respectively. However, there is considerable room for future improvements—Kerr combs have been demonstrated with a threshold power as low as 50 μW in silica toroids[2]. In general, the threshold for Kerr comb generation scales inverse-quadratically with the Q-factor of the resonator[21]. A tenfold Q-factor improvement would lead to a reduction of the threshold pump power by a factor of 100, and the 2 W pump laser could be replaced by a 20 mW pump laser diode[2].

Feedback stabilization of a Kerr comb. To maintain low-phase-noise comb states during an extended data transmission experiment, it is important to keep the pump conditions as constant as possible. In the first experiment, we found that the on-chip pump power was a crucial parameter and had to be kept constant to approximately ±5% to maintain thermal locking of the cavity resonance to the pump wavelength[30]. The second experiment relied on stable comb generation for extended studies of data transmission performance. This was achieved by an independent control loop based on commercially available hardware (Melles Griot NanoTrak), which kept the lensed fibres in the optimum coupling position. We also implemented a second control loop using a commercially available proportional-integral-derivative (PID) controller (TEM Messtechnik LaseLock), which used the power in the comb lines as a feedback signal and controlled the pump laser detuning such that thermal drifts of the resonator were followed by a slight adaptation of the pump wavelength (see Supplementary Section I for a more detailed discussion). The combination of these two control loops enabled stable Kerr comb operation over several hours without manual interaction.

Received 17 July 2013; accepted 27 February 2014; published online 13 April 2014

References

1. Hillerkuss, D. *et al.* 26 Tbit s^{-1} line-rate super-channel transmission utilizing all-optical fast Fourier transform processing. *Nature Photon.* **5,** 364–371 (2011).
2. Del'Haye, P. *et al.* Optical frequency comb generation from a monolithic microresonator. *Nature* **450,** 1214–1217 (2007).
3. Levy, J. *et al.* High-performance silicon-nitride-based multiple-wavelength source. *IEEE Photon. Technol. Lett.* **24,** 1375–1377 (2012).
4. Herr, T. *et al.* Universal formation dynamics and noise of Kerr-frequency combs in microresonators. *Nature Photon.* **6,** 480–487 (2012).
5. Pfeifle, J. *et al.* in *Optical Fiber Communication Conference*, paper OW1C.4 (Optical Society of America, 2012).
6. Wang, P.-H. *et al.* Observation of correlation between route to formation, coherence, noise, and communication performance of Kerr combs. *Opt. Express* **20,** 29284–29295 (2012).
7. Herr, T. *et al.* Temporal solitons in optical microresonators. *Nature Photon.* **8,** 145–152 (2014).
8. Li, J., Lee, H., Chen, T. & Vahala, K. J. Low-pump-power, low-phase-noise, and microwave to millimeter-wave repetition rate operation in microcombs. *Phys. Rev. Lett.* **109,** 233901 (2012).
9. Okawachi, Y. *et al.* Octave-spanning frequency comb generation in a silicon nitride chip. *Opt. Lett.* **36,** 3398–3400 (2011).

10. Miller, D. Device requirements for optical interconnects to silicon chips. *Proc. IEEE* **97,** 1166–1185 (2009).
11. Qian, D. *et al.* in *Optical Fiber Communication Conference*, paper PDPB5 (Optical Society of America, 2011).
12. Hochberg, M. & Baehr-Jones, T. Towards fabless silicon photonics. *Nature Photon.* **4,** 492–494 (2010).
13. Liu, A. *et al.* Wavelength division multiplexing based photonic integrated circuits on silicon-on-insulator platform. *IEEE J. Sel. Top. Quant.* **16,** 23–32 (2010).
14. Feng, D., Qian, W., Liang, H., Luff, J. & Asghari, M. High speed receiver technology on the SOI platform. *IEEE J. Sel. Top. Quant.* **19,** 3800108 (2013).
15. Nagarajan, R. *et al.* InP photonic integrated circuits. *IEEE J. Sel. Top. Quant.* **16,** 1113–1125 (2010).
16. Park, H., Fang, A., Kodama, S. & Bowers, J. Hybrid silicon evanescent laser fabricated with a silicon waveguide and III–V offset quantum wells. *Opt. Express* **13,** 9460–9464 (2005).
17. Witzens, J., Baehr-Jones, T. & Hochberg, M. Silicon photonics: on-chip OPOs. *Nature Photon.* **4,** 10–12 (2010).
18. Hillerkuss, D. *et al.* Single-laser 32.5 Tbit/s Nyquist WDM transmission. *J. Opt. Commun. Netw.* **4,** 715–723 (2012).
19. Wu, R., Supradeepa, V. R., Long, C. M., Leaird, D. E. & Weiner, A. M. Generation of very flat optical frequency combs from continuous-wave lasers using cascaded intensity and phase modulators driven by tailored radio frequency waveforms. *Opt. Lett.* **35,** 3234–3236 (2010).
20. Rosales, R. *et al.* InAs/InP quantum-dot passively mode-locked lasers for 1.55-μm applications. *IEEE J. Sel. Top. Quant.* **17,** 1292–1301 (2011).
21. Kippenberg, T. J., Holzwarth, R. & Diddams, S. A. Microresonator-based optical frequency combs. *Science* **332,** 555–559 (2011).
22. Savchenkov, A. A. *et al.* Tunable optical frequency comb with a crystalline whispering gallery mode resonator. *Phys. Rev. Lett.* **101,** 093902 (2008).
23. Razzari, L. *et al.* CMOS-compatible integrated optical hyper-parametric oscillator. *Nature Photon.* **4,** 41–45 (2010).
24. Levy, J. S. *et al.* CMOS-compatible multiple-wavelength oscillator for on-chip optical interconnects. *Nature Photon.* **4,** 37–40 (2010).
25. Lindenmann, N. *et al.* Photonic wire bonding: a novel concept for chip-scale interconnects. *Opt. Express* **20,** 17667–17677 (2012).
26. Dong, P., Chen, L., Xie, C., Buhl, L. L. & Chen, Y.-K. 50-Gb/s silicon quadrature phase-shift keying modulator. *Opt. Express* **20,** 21181–21186 (2012).
27. Korn, D. *et al.* Silicon-organic hybrid (SOH) IQ modulator using the linear electro-optic effect for transmitting 16QAM at 112 Gbit/s. *Opt. Express* **21,** 13219–13227 (2013).
28. Schmogrow, R. *et al.* Real-time Nyquist pulse generation beyond 100 Gbit/s and its relation to OFDM. *Opt. Express* **20,** 317–337 (2012).
29. Essiambre, R.-J., Kramer, G., Winzer, P., Foschini, G. & Goebel, B. Capacity limits of optical fiber networks. *J. Lightwave Technol.* **28,** 662–701 (2010).
30. Carmon, T., Yang, L. & Vahala, K. Dynamical thermal behavior and thermal self-stability of microcavities. *Opt. Express* **12,** 4742–4750 (2004).

Acknowledgements

This work was supported by the European Research Council (ERC starting grant 'EnTeraPIC', no. 280145), the Alfried Krupp von Bohlen und Halbach Foundation, the Helmholtz International Research School for Teratronics (HIRST), the EU-FP7 project BigPipes, the Initiative and Networking Fund of the Helmholtz Association, the Center for Functional Nanostructures (CFN) of the Deutsche Forschungsgemeinschaft (DFG) (project A 4.8), the DFG Major Research Instrumentation Programme, the Karlsruhe Nano-Micro Facility (KNMF), the Karlsruhe School of Optics & Photonics (KSOP), the Swiss National Science Foundation (NCCR Nano-Tera, NTF MCOMB), the Marie Curie IAPP Action, the Defense Advanced Research Projects Agency (DARPA) via the QuASAR programme and the European Space Agency (ESA) via a doctoral fellowship (to V.B.). Samples were fabricated at the EPFL Center for Micro- and Nanotechnology (CMi).

Author contributions

J.P. conceived and performed the data transmission experiments and analysed the data. V.B. and K.H. conceived, designed and fabricated the devices, which were characterized jointly by V.B. and T.H. M.L., Y.Y., D.W., P.S. and C.W. performed the data transmission experiments and analysed the data. The feedback stabilization of the comb source for the second experiment was implemented jointly by J.P. and Y.Y. J.Li, D.H. and R.S. contributed subsystems to the data transmission experiments. The project was supervised by R.H., W.F., J.L., T.J.K. and C.K. T.J.K. conceived and supervised the comb generation scheme and fabrication of the devices, C.K. conceived the data transmission and comb stabilization schemes and supervised the experiments. All authors discussed the data and wrote the manuscript jointly.

Additional information

Supplementary information is available in the online version of the paper. Reprints and permissions information is available online at www.nature.com/reprints. Correspondence and requests for materials should be addressed to T.J.K. and C.K.

Competing financial interests

The authors declare no competing financial interests.